Towards chemical identification in atomic-resolution noncontact AFM imaging with silicon tips

A. S. Foster
Laboratory of Physics, Helsinki University of Technology, P.O. Box 1100, FIN-02025, Finland

A. Y. Gal
Department of Physics and Astronomy, University College London, Gower Street, London WC1E 6BT, United Kingdom

J. M. Airaksinen, O. H. Pakarinen, and Y. J. Lee
Laboratory of Physics, Helsinki University of Technology, P.O. Box 1100, FIN-02025, Finland

J. D. Gale
Department of Chemistry, Imperial College London, Exhibition Road, London SW7 2AZ, United Kingdom

A. L. Shluger
Department of Physics and Astronomy, University College London, Gower Street, London WC1E 6BT, United Kingdom

R. M. Nieminen
Laboratory of Physics, Helsinki University of Technology, P.O. Box 1100, FIN-02025, Finland
(Received 27 June 2003; published 24 November 2003)

In this study we use *ab initio* calculations and a pure silicon tip to study the tip-surface interaction with four characteristic insulating surfaces: (i) the narrow gap TiO_2 (110) surface, (ii) the classic oxide MgO (001) surface, (iii) the ionic solid $CaCO_3$ $(10\bar{1}4)$ surface with molecular anion, and (iv) the wide gap CaF_2 (111) surface. Generally we find that the tip-surface interaction strongly depends on the surface electronic structure due to the dominance of covalent bond formation with the silicon tip. However, we also find that in every case the strongest interaction is with the highest anion of the surface. This result suggests that, if the original silicon tip can be carefully controlled, it should be possible to immediately identify the species seen as bright in images of insulating surfaces. In order to provide a more complete picture we also compare these results to those for contaminated tips and suggest how applied voltage could also be used to probe chemical identity.

DOI: 10.1103/PhysRevB.68.195420 PACS number(s): 68.37.Ps, 73.90.+f, 68.47.Gh, 07.05.Tp

I. INTRODUCTION

As the sophistication and reliability of noncontact atomic force microscopy (AFM) techniques increase,[1] the obtained physical information is greatly expanded from topographical images alone. This is seen particularly in the recently demonstrated ability to produce force vs distance curves over specific sites in atomically resolved images at low temperatures[2–4] (and hopefully soon at room temperature[5]). Access to this level of *force resolution* greatly increases the possibilities of comparison between theory and experiment,[3,6,7] and, hence, leads to greater understanding of the tip-surface interaction. However, this has not yet significantly impacted the long-standing problem of establishing directly the chemical identity of surface species in atomically resolved images. This is largely due to a very strong dependence of images on the precise atomistic structure of the tip apex responsible for the image contrast. Since this structure is unknown, the existing attempts at quantitative interpretation of experimental images are either based on extensive simulation using model tips (e.g., Refs. 8 and 9) or via analysis of force curves.[3] In particular, previous simulations of AFM imaging on insulating surfaces assumed the tip would be oxidized or contaminated, and hence have been performed mainly with model ionic oxide tips.[10,1] Imaging silicon, one can assume that tip can be terminated by silicon atoms, and indeed modeling with a silicon tip with a dangling bond at the apex led to reasonable agreement between measured and calculated forces.[11,1] There have been several studies where both pure silicon tips and those contaminated by surface atoms were used to calculate the interaction with surfaces other than Si, e.g., TiO_2,[12,13] GaAs,[14,15] InP,[16,17] and CaF_2.[6] However, quantitative comparison with experiment has been possible only in very few cases.[3,6]

The growing possibilities for direct comparison of measured and calculated force vs distance curves above particular surface sites open new opportunities for testing tip models and hence determining the chemical identity of image features. When used systematically in conjunction with theoretical modeling, such comparison may provide fingerprints necessary for discriminating different tip structures.[6] Since most tips are made from silicon, this tip seems a natural starting point for building a database of tip-surface interactions for ''realistic'' tip structures. Some preliminary results on the interaction of a Si tip with a dangling bond at the apex Si atom with several insulators have been presented in Ref. 18. In this study, we attempt to show systematically how the Si tip-surface force depends on the tip and surface electronic structure for several different types of insulating surfaces: TiO_2, MgO, $CaCO_3$, and CaF_2. We use a reactive silicon tip model to show how the balance between polarization and covalent contributions to the force depends on the surface

electronic structure. The strongest interaction for this tip is always with the surface anion and thus the source of image contrast is immediately evident. We also demonstrate that by applying voltage to change externally the tip and surface electronic structure, one can control the tip-surface interaction, which provides a further way of identifying the character of the atom under the tip. Therefore further advances in preparation and control over Si tips could help solving the problem of chemical identity of image features.

On insulators, reactive silicon tips can be easily contaminated by surface or ambient oxygen atoms and even by clusters of surface atoms. We therefore compare the results for the Si tip with those obtained for a MgO cluster tip model representing a more strongly contaminated or originally oxide tip. The ''trademark'' of this tip is a strong electrostatic interaction with the surface ions. Surprisingly, the magnitude of force acting on this tip appears to be very similar to that calculated for the Si tip model. We conclude by discussing the mechanisms of the tip-surface interaction for different tip types and their effect on the image contrast.

II. METHODS

The majority of the modeling in this study was performed using a model of a pure silicon tip consisting of a ten-atom silicon cluster with a single dangling bond at the apex and its base terminated by hydrogen.[19,18] This tip is produced by taking three layers from the Si (111) surface, and removing atoms to produce a sharp apex. It provides a fair model of the dangling bond, characteristic of the most stable (7×7) reconstruction of the Si (111) surface. The highest occupied molecular orbital (HOMO) of the tip, representing the dangling bond, is quite diffuse and will overlap simultaneously with several surface ions.[18] The corresponding one-electron state is split from other occupied states of the Si tip modeling the Si valence band. The small size, specific shape, and hydrogen termination of the tip produce a surface electronic structure different from a standard silicon surface. However, this tip performs well when the short-range tip-surface interaction is determined by the onset of covalent bond formation between the dangling bond at the end of the tip and surface dangling bonds. This has been demonstrated by the good agreement of calculated and measured forces over a silicon surface.[3]

For comparative purposes, calculations were also made using an ionic oxide tip model—a 64-atom MgO cube, orientated symmetrically around the *z* axis, with a single Mg atom at the lower apex. The Mg-terminated MgO tip produces a net positive electrostatic potential towards the surface. Compared to the Si tip, it is also much more rigid and, hence, tip relaxation is much less significant. The strength of the tip-surface interaction for this tip is determined by the Coulomb interaction with the surface ions and has been shown to agree with experiment where tip contamination by an ionic material is probable.[9]

All calculations with the Si tip were performed using the linear combination of atomic orbitals basis SIESTA code,[20,21] which implements density-functional theory (DFT) in a manner so as to achieve linear scaling in the construction of the Hamiltonian and overlap matrices. Solution of the self-consistent problem can also be performed with linear scaling for insulators, though here full diagonalization is employed so that the electronic structure of the surfaces can be studied in detail. The generalized gradient approximation has been utilized in all calculations, based on the specific functional of Perdew, Burke, and Ernzerhof.[22] Core electrons are represented by norm-conserving pseudopotentials of the form proposed by Troullier and Martins,[21] and we used the partial core correction scheme of Louie *et al.*[23] The pseudopotential for the silicon atom was generated in the electron configuration $[\mathrm{Ne}]3s^2\ 3p^2$, for calcium in $[\mathrm{Ar}]4s^2$, carbon in $[1s^2]2s^2 2p^2$, oxygen in $[1s^2]2s^2 2p^4$, titanium in $[\mathrm{Ar}]4s^2 3d^2$, fluorine in $[1s^2]2s^2 2p^5$, and that for magnesium in $[\mathrm{Ne}]3s^2$ configuration, where square brackets denote the core electron configurations. Various basis set configurations were tested, and a good compromise between accuracy and efficiency was found for the following sets: CaF_2 (double ζ for F and triple ζ with double polarization for Ca); $CaCO_3$ (double ζ with polarization for all); TiO_2 (double ζ with polarization for Ti and triple ζ with polarization for O); and MgO (double ζ for Mg and double ζ with polarization for O). Double ζ with polarization was used for Si and H in the tip in all cases. All calculations were converged to the order of meV in the total energy with respect to mesh cutoff and orbital cutoffs (i.e., energy shift[21]). The following energy shifts and mesh cutoff values were used: CaF_2(50 meV, 255 Ry.); $CaCO_3$ (25 meV, 156 Ry.); TiO_2 (15 meV, 126 Ry.); and MgO (14 meV, 159 Ry.). Within these limits all the properties of the silicon tip are well converged. Energy convergence with respect to *k*-point sampling was also tested on calculations of accurate surface geometries using smaller slabs, but for the large tip-surface systems only the γ point was used. However, the surface structure did not change significantly between the small and large systems. During simulations the top half of the tip and the bottom third of the surface were kept frozen, and all other ions were allowed to relax freely to less than 0.05 eV/Å. Calculated surface geometries provided good agreement with experimental surface relaxations, and were converged with respect to slab thickness. We did not consider a full spin-polarized treatment of the problem since previous studies using similar[12] and identical methods[18] indicate that it does not make a qualitative difference to the results.

The MgO tip calculations were performed using atomistic simulations and the MARVIN2 code.[24,25] This technique uses point charges in order to represent ions and the shell-model representation of ion polarization, where appropriate, while empirically fitted potentials, are used to calculate interatomic interactions. The force field parameters for the systems discussed in this work have been taken from previous publications: MgO;[10] $CaCO_3$;[26] CaF_2;[8] and TiO_2.[27] To test electronic effects, SIESTA calculations have been performed also for the MgO tip and the MgO (001) surface, and reasonable agreement was achieved.

III. SURFACE PROPERTIES

The four surfaces which we will consider in this study are the following: the TiO_2 (110) surface; the $CaCO_3$ $(10\bar{1}4)$

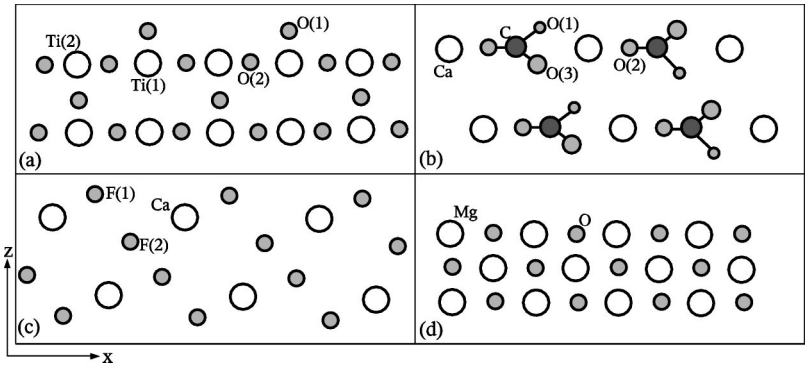

FIG. 1. Side cross sections in the *x*-*z* (where *z* is the surface normal direction) plane of the atomic structures of surfaces considered in this study: (a) TiO_2 (110), (b) CaF_2 (111), (c) $CaCO_3$ $(10\bar{1}4)$, and (d) MgO (001). Note that the oxygen atoms in $CaCO_3$ have been drawn in perspective.

surface; the CaF_2 (111) surface; and the MgO (001) surface. Each has wide technological applications and a long history in surface science, but they have also been the subject of several noncontact AFM studies.[1] The structures of these surfaces are summarized in Fig. 1, and discussed briefly below.

The TiO_2 (110) surface [Fig. 1(a)] is oxygen terminated with the bridging oxygen rows [O(1)] protruding about 0.1 nm above the surface plane. The titanium ions [Ti(1)] are positioned between bridging oxygens and are bonded to two of the four in-plane oxygens [O(2)] between which the more exposed Ti(2) ions are situated. A periodic cell of $(4\times4\times3)$ TiO_2 units was used to simulate the surface in our calculations.

The $CaCO_3$ $(10\bar{1}4)$ surface is more complex due to the fact that this crystal could be considered as a molecular solid. In principle it is oxygen terminated, with the O(1) [see Fig. 1(b)] protruding about 0.09 nm from the surface plane. However, this oxygen belongs to a CO_3^{2-} molecular ion, with one oxygen [O(2)] in plane with the Ca and C atoms, and one [O(3)] below them. The surface unit cell also requires two $CaCO_3$ groups, since alternating rows of CO_3 groups along the [010] direction are rotated about a surface normal, forming a zigzag of O(1) atoms along the $[\bar{4}\bar{2}1]$ direction.[1] This surface was modeled by a periodic slab containing $(3\times4\times3)$ $CaCO_3$ units in our calculations. While there have been experimental low-energy electron-diffraction observations of a (2×1) reconstruction under certain conditions,[28] which have been recently supported by computer simulation,[29] we postpone discussion of this subtle effect for later work.

The CaF_2 (111) surface is fluorine terminated, with the high fluorine atoms [F(1) in Fig. 1(c)] protruding by about 0.08 nm from the Ca sublattice, with the low fluorine atoms [F(3)] a similar distance below. Here the surface is represented by a periodic cell of $(4\times4\times3)$ CaF_2 units.

Finally, the MgO (001) surface, which contains only two sublattices [see Fig. 1(d)], was simulated using a periodic cell of $(6\times3\times3)$ MgO units. The validity of the general method and system size to treat these surfaces has been thoroughly tested via comparison to experiment and previous calculations wherever possible. The results of these tests are presented elsewhere since they are not the focus of this work.[1,9,18,13] Note that in the following discussion, the plane formed by the highest atoms in the surface is used as a zero plane for determining the tip-surface distance.

To study the dependence of the tip-surface interaction on the surface electronic structure, we considered four different insulators. Although they are all in principle insulators, the electronic structure of the four materials studied in this paper differs markedly, which is of course the reason whey they are being studied (see Table I). TiO_2 is a narrow gap insulator (or wide gap semiconductor), with a calculated band gap (E_g) of 0.6 eV, compared to an experimental value of 3.0 eV.[30] Despite the strong covalent bonding in the CO_3 group, overall $CaCO_3$ is a fairly wide gap insulator with a calculated band gap of 5.0 eV (6.0 eV, expt., Ref. 31), and strongly ionic Ca^{2+} and CO_3^{2-} sublattice. In this company, CaF_2 represents a classic wide gap ionic insulator, with a band gap of 6.6 eV (12.3 eV, expt., Ref 32). MgO is also a classic wide gap insulator, but its band gap of 3.6 eV (7.8 eV, expt., Ref 33) is significantly smaller than CaF_2. Note that in the following discussion, the large difference between theoretical and experimental band gaps is a systematic error of the DFT method, and cannot be corrected easily. However, the ground-state geometric and electronic structures of these crystals are well reproduced in DFT, so this error does not affect the conclusions we discuss here.

In the following discussion we correlate the covalent bonding contributions to the tip-surface interaction with the electron-density transfer between the tip and surface (characterized by Mulliken charges), and with the valence-band offset with the tip HOMO state. The charge transfer is calculated by summing all the Mulliken charges in the tip and

TABLE I. Various *ab initio* calculated properties of the surfaces in this study: band gap (E_g); Mulliken charge on the cations (Q_{cation}); average Mulliken charge on the anions (Q_{anion}); valence-band offset between silicon tip and surface at large separation (VB_{off}). Note that the fact that cation and anion charges for $CaCO_3$ and TiO_2 are different is due to charge variations between anion sublattices and changes in charge as a function of position in the slab—overall charge is conserved, and these numbers represent an average indicator.

Material	E_g (eV)	Q_{cation}	Q_{anion}	VB_{off} (eV)
TiO_2	0.6	+0.9	−0.4	−0.5
$CaCO_3$	5.0	+1.7	−1.8 (CO_3)	0.4
CaF_2	6.6	+1.6	−0.8	3.0
MgO	3.6	+1.6	−1.6	−0.7

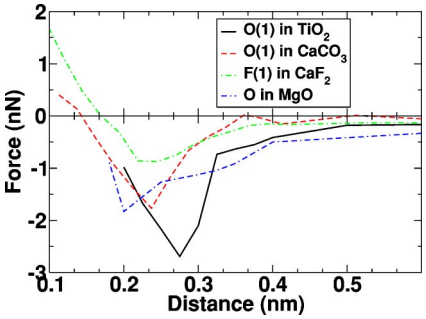

FIG. 2. Forces with a silicon tip over anion sites for each of the surfaces studied. The labels in the legend refer to Fig. 1. Note that the lack of smoothness in the force curves is due to the limited number of points calculated and the atomic force tolerance used in relaxations.

surface at the relevant tip-surface separation, and comparing this with a reference calculation with the tip at 2 nm from the surface. This should be analytically equivalent [assuming infinite accuracy in the partial DOS (PDOS) and after normalization] to integrating over all the tip and surface states of the PDOS, and comparisons between this and Mulliken summing gave very good agreement if the PDOS was calculated to a high enough accuracy. The offset is evaluated directly from the PDOS with the tip far ($\sim$2 nm) from the surface, and is defined as the difference between the tip HOMO (dangling bond state) and the surface HOMO (valence-band edge). Not unexpectedly, CaF_2 has the largest offset from the silicon tip of the materials studied here (3.0 eV), and therefore one would expect the smallest amount of charge transfer. The calculated offsets for other materials are much smaller (see Table I) and one should expect much more charge transfer as the tip approaches. The band offset itself is also a function of distance, and in the case of CaF_2 changes from 3.0 eV at 2 nm to 3.4 eV at 0.4 nm and to 4.2 eV at 0.3 nm.

IV. TIP-SURFACE INTERACTION

In order to understand how the properties of the surfaces and tips discussed above affect the tip-surface interaction, we study how the force on the tip depends on distance above two sublattices on each surface: one anion and another cation. Since we are interested mainly in qualitative conclusions, these will not change significantly over the other sublattices. We will also compare the forces for the silicon tip and the oxide tip to demonstrate how different interaction regimes affect the properties of the force.

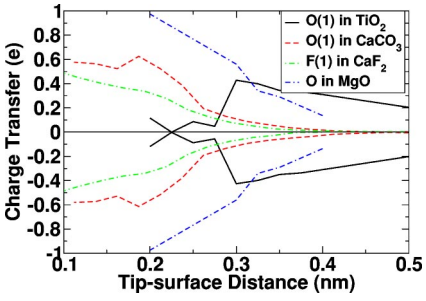

FIG. 3. Charge transfer from the surface (negative) to silicon tip (positive) as the tip approaches the surface over an anion site. Note that for TiO_2 the charge is transferred from the tip to the surface.

A. Si tip

In general, we expect the force between a silicon tip and the surface to have two main components: (i) an onset of covalent bonding between the tip and the surface, which should be mainly dominated by the atom directly under the tip, but may have contributions from other atoms and (ii) the weaker force due to the polarization of the tip by the ionic insulating surface. The contribution of each of these components to the tip-surface interaction should depend strongly on the electronic structure of the surface. Also, the polarization of the tip should depend on the formal charge of the surface ions, such that a doubly charged ion induces a larger effect than a singly charged one.

Figure 2 shows the forces over anion sites in each surface with a silicon tip. We see immediately that the largest overall force occurs over the O(1) site in the TiO_2 surface, with a smaller force for O in MgO and O(1) in $CaCO_3$. The smallest force is found for F(1) in CaF_2. If the full range of interaction is considered, it can also be seen that the force has a much longer range for MgO and TiO_2, with over double the force for the other surfaces in the 0.3–0.4 nm distance range. This marked difference in the interaction is directly related to the ability of the Si tip to make a semicovalent bond with the surface ions. This effect can be characterized by the electron-density transfer between the tip and the surface as a function of distance and is presented in Fig. 3.

As one can see in Fig. 3, for CaF_2, there is very little charge transfer until very close approach is achieved, and when charge transfer does occur (below 0.25 nm) the tip has already entered the repulsive interaction regime. This correlates with the large energy offset of the tip dangling bond state and the top of the surface valence band (see Table I). Furthermore, the singly charged fluorine ions produce only weak polarization compared to the doubly charged ions in $CaCO_3$ and MgO. Correspondingly for $CaCO_3$ the increased charge transfer and polarization produces an increase in force (for example, a large increase in both charge transfer and force relative to CaF_2 can be observed at around 0.25 nm). This again correlates with the strongly reduced offset energy for $CaCO_3$ comparing to CaF_2.

In MgO the small offset means that there is significant charge transfer at longer ranges, over 0.2*e* already at 0.4 nm, and this increases almost linearly as the tip approaches the surface. This produces the much larger force compared to CaF_2 and $CaCO_3$ in the 0.3–0.4 nm range. Below 0.3 nm we see that the force over MgO and $CaCO_3$ is very similar, despite the large difference in charge transfer. This can be caused by the much stronger distortion of the softer $CaCO_3$ surface induced by the interaction with the tip (see also Ref. 34).

Our results for TiO_2 agree qualitatively with a previous *ab initio* study,[12] in that the largest force is generally seen over the bridging oxygen sites. However, we observe significantly

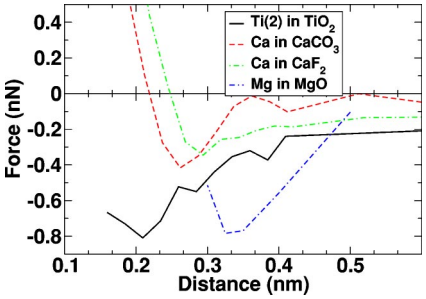

FIG. 4. Forces with a silicon tip over cation sites for each of the surfaces studied.

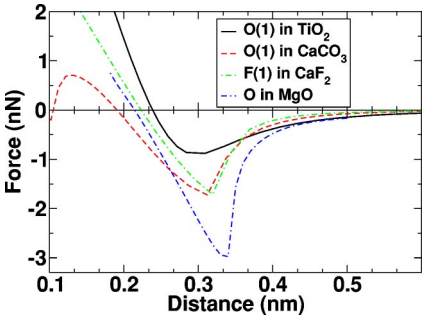

FIG. 6. Forces with an oxide tip over anion sites for each of the surfaces studied.

smaller forces and a different range of interaction—this maybe related to the simplistic one silicon atom tip they used in that study and will be investigated in detail in a later work.[13] Due to its small band gap and small offset, in the TiO_2 surface we find a completely different story from the other surfaces. Charge is now actually transferred from the tip to the surface—the magnitude of transfer is comparable to that for MgO and so similar forces are seen in the 0.35 nm–0.50 nm range. This transfer to the surface increases its ionicity and produces a stronger polarization effect, producing the largest force for any surface at around 0.275 nm.

The difference in the direction of charge transfer for TiO_2 is a consequence of the different surface electronic structures—specifically the nature of the valence band (VB) and conduction band (CB). For the most ionic surface, CaF_2, the VB is almost exclusively F *p* states and the CB Ca *s* states, while for $CaCO_3$ the VB is dominated by O *p* states and the CB by Ca *s*-states. There are basically no unoccupied states on the anions, so effective charge transfer can only be to the tip. For MgO there is an admixture of Mg and O states in the VB, with the top of the valence band of purely oxygen character. However, this admixture is much smaller in the CB, and the transfer direction remains to the tip. TiO_2 has the largest admixture of states of any surface, reflecting the significant covalence of the Ti-O bonds and the CB has a significant fraction of unoccupied O *p* states. Hence bonding between the tip and anion sites in the TiO_2 surface involves effective charge transfer to the surface.

Turning now to consider the forces over cation sites with a silicon tip (see Fig. 4), they are generally much smaller than the corresponding forces over the anion site. This agrees with the consistent reduction in charge transfer shown in Fig. 5. The cations, especially in the more ionic surfaces, have already donated much of their charge to the anions and there is little remaining, i.e., there are no occupied cation states in the VB to provide electrons and it is not energetically favorable to transfer charge from the tip to cation unoccupied states in the CB. The general trends also match those for the anion curves, with large forces and charge transfer for the less ionic MgO and TiO_2 surfaces. For MgO, significant VB states with Mg character exist, so this, and the interaction with neighboring oxygens results in larger charge transfer. We again see charge transfer from the tip to surface for TiO_2, in contrast to the other surfaces. However, the system charge density shows that no strong bonds are formed with the Ti in the surface, and that the interaction is due to the surrounding oxygen atoms, and has a similar source to the interaction seen over oxygen.

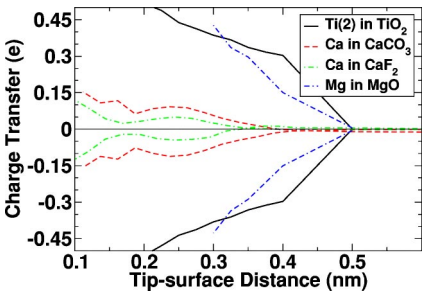

FIG. 5. Charge transfer from silicon tip (positive) to surface (negative) as the tip approaches the surface over a cation site. Note that for TiO_2 the charge is transferred from the tip to the surface.

A common feature in Figs. 2 and 4 is the onset of repulsion at small tip-surface distances, i.e., less than 0.3 nm. This is due to electron-electron repulsion as tip and surface orbitals begin to overlap. At this point the tip is no longer really in the noncontact regime and has entered the contact regime. At such small distances, the surface atoms are pushed into the surface and the apex Si atom undergoes strong relaxation back into the tip cluster. Hence, the tip-surface distance in Figs. 2 and 4 is slightly misleading, and the real distance between the tip and surface is much larger, e.g., for the tip over F(1) in CaF_2 at a tip-surface distance of 0.1 nm, the real distance between the F(1) ion, and the tip apex was 0.19 nm due to a relaxation of -0.04 nm by F into the surface and $+0.05$ nm by Si into the tip. Obviously atomic relaxation plays a role at all distances,[9,10] but it is only at close range that it's magnitude becomes comparable to the tip-surface separation. At these small tip-surface separations, the accuracy of the charge-transfer values are also more difficult to estimate. As the tip approaches the surface, bonding changes the PDOS from a simple "tip+surface picture," and therefore assigning charges to specific atoms becomes much more inaccurate.

B. MgO tip

Our SIESTA calculations for the MgO tip interacting with the MgO (001) surface demonstrate that for an oxide tip,

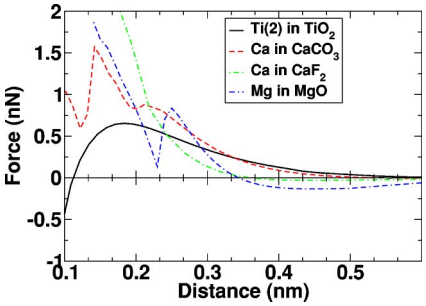

FIG. 7. Forces with an oxide tip over cation sites for each of the surfaces studied.

charge transfer is generally minimal, and the force should be dominated by the electrostatic interaction between the tip and surface. Therefore to model the interaction of the oxide tip with different surfaces we employ an atomistic simulation technique, which excludes charge transfer completely. The forces over oxygen sites for the positively terminated oxide tip (see Fig. 6) are easily defined by the surface geometry and the relative effective charges of the anions, since these determine the strength of the electrostatic potential at that point. The strongest interaction is for oxygen in MgO, where the highly charged O^{2-} ion produces a force almost double that of any other surface. We have compared this atomistic simulation result directly with an *ab initio* calculation of the same system, and found that the force agrees to within 20%.

This means that although the atomistic simulations exaggerate the ionic charge (-2.0 compared to -1.6 in Table I), this merely compensates for excluding any charge-transfer processes and the method is quite accurate. We see the largest force over the doubly charged O^{2-} in MgO, then a reduction by about a factor of 2 to the singly charged F^- ion in CaF_2. Over the high O in calcite, the tip is effectively interacting with three $O^{-1.045}$ ions surrounding a single $C^{+1.135}$ ion in the carbonate group, and this produces a force comparable to that over F^-. Finally, over oxygen in TiO_2, the electrostatic interaction with the $O^{-1.098}$ is compensated by a long-range repulsive component, giving the smallest force—as appropriate for this least ionic material.

The forces for cation sites with an oxide tip are the most uniform of all configurations studied. The forces are all small, and very rapidly tending to repulsion—as would be expected for the interaction of a positively terminated tip above a cation site. At a very close approach, it is observed that there are rapid changes in the force, characteristic of extreme displacements and jumps of ions under the tip. For the more strongly bonded Ti in TiO_2, these jumps are not observed and a smooth repulsive force is observed until the tip begins to also strongly interact with surface oxygens.

We have also calculated the interactions of an O terminated MgO tip with a net negative electrostatic interaction over the same surfaces, but the interaction physics is the same as for the Mg-terminated tip, but with cations dominating the interaction such that Figs. 6 and 7 would be more or less reversed.

TABLE II. Force and charge transfer to the tip (Q) for various applied electrostatic fields (E) when the tip is at 0.4 nm above Ca and F(1) sites in the CaF_2 surface. A positive electrostatic field means that the field increases with increasing *z*.

E (V/Å)	Ca		F(1)	
	Force (nN)	Q (e)	Force (nN)	Q (e)
0.0	−0.26	+0.01	−0.40	+0.05
−0.5	−0.08	−0.32	−0.02	−0.33
+0.5	−0.06	+0.38	−0.67	+0.47

V. VOLTAGE EFFECTS

The results of the preceding section demonstrate that by controlling the nature of the tip we can immediately tell the source of contrast. For example, if it is a silicon tip, then the strongest interaction will be with the surface anions. However, this implies a level of tip regulation as yet not seen often in AFM, and it is important to explore other possible methods for identifying the atom under the tip. The sensitivity of the tip-surface interaction to the surface electronic structure shown here implies that if we can change that structure systematically then the change in the tip-surface interaction should tell us the identity of the atom under the tip. The most obvious way to change the surface electronic structure, and especially the energy offset between the tip dangling bond and the surface valence band, VB_{off}, is by applying a voltage across the system. This is a common practice in AFM experiments, but may prove particularly useful when imaging thin films on conducting substrates with conducting Si tips.

As a first approximation to studying the effects of voltage in such a system, we have applied an electrostatic potential gradient to our supercell in the direction normal to the surface.[21] The field is applied in such a way that the discontinuity in the gradient between different images is always in the vacuum,[35] and it does not affect the results. To demonstrate the possibilities of this idea, we have studied the surface where charge-transfer effects were smallest—the CaF_2 surface. The system setup is exactly the same as for the silicon tip calculations discussed previously, but now the atoms are relaxed in the presence of the electrostatic field.

Table II shows how the force and charge transfer change at one height as the electrostatic field is applied. Over the cation site, we see a field applied in either direction reduces the overall force, despite producing strong charge transfer in opposite directions. For the anion site, the force is strongly reduced when the field decreases with increasing *z*, but it is significantly increased when the field increases with increasing *z* (where *z* is the surface normal direction). The charge transfer changes correspondingly. The +0.5 V field also results in a very large displacement of the F atom by 0.13 nm towards the tip—it effectively jumps to the tip. In general, the atom under the tip experiences a double-well potential,[36] with energy minima near to the surface and near to the tip separated by a barrier dependent on the tip-surface distance. Applying a large enough voltage means the surface atom can

overcome the barrier and jump to the tip. In all the other cases the displacements of the tip and surface atoms are less than 0.01 nm.

The dramatic difference in behavior between the cation and anion sites can be understood readily from the discussion of the contributions to the tip-surface interaction in the previous sections. Over the anion site, the force is dominated by the charge transfer from the ion to the tip, and a positive applied bias encourages this while a negative bias reverses it, changing the force accordingly. For the cation, the preceding section demonstrated that charge transfer is a smaller component to the tip-surface interaction than for anions, and the force is dominated by the polarization of the tip. At negative bias, the extra charge on the cation reduces the polarization interaction with the tip and therefore the force. However, for positive applied bias, charge actually transfers from the surrounding anion lattice, not the cation under the tip. Hence, there is still no formation of any strong covalent bonds, but again the ionicity of surface ions and the contribution of tip polarization to the interaction are reduced. This behavior is also observed for a 0.375 nm tip-surface distance, although the effect is slightly diminished.

This contrasting behavior of cations and anions in the surface suggests a possible method for chemical identification during an AFM experiment. By producing experimental force vs distance curves over different atomic sites in the surface at equal and opposite bias it should be possible to immediately tell which is an anion and which is a cation. This process would involve subtracting the positive bias curve from the negative bias curve at the same site to remove the background forces (applying a bias will change the background capacitance force and mask the real change in chemical forces), and then looking at the two differential curves. The curve where the difference is largest, i.e., where changing the bias had the biggest effect, should be the anion set. Obviously the difference between differential curves will depend on the surface studied and the nature of the tip, and one would suspect that this method will work best on very ionic surfaces. Furthermore, in the event that the tip is really pure silicon then the interpretation should be easily made according to the results of the preceding section. This more complex approach, involving a bias voltage, is more relevant to the situation where there is uncertainty regarding the nature of the tip, e.g., after a tip crash. However, as we have shown in the preceding section, the general principle is relevant across surfaces with very different electronic structures, and therefore definitely requires further investigation.

VI. DISCUSSION

We have studied the interaction of two model tips with several insulating surfaces having different geometric and electronic structures. The results of *ab initio* calculations for a silicon tip demonstrate that the contributions to the tip-surface force can be related to the nature of the surface electronic structure. Wide gap insulators are generally very ionic, with a large valence-band offset preventing significant electron-density transfer between tip and surface, and the force is dominated by polarization of the tip. As the gap and ionicity is reduced, the charge-transfer increases and onset of covalent bonding soon begins to dominate the tip-surface interaction, producing much larger forces overall. The forces over anions in the surface are larger than over cations, as they play a more significant role in charge transfer processes—especially in the more ionic surfaces. This implies that if a Si tip with a dangling bond can be prepared and maintained, image interpretation becomes almost trivial. For a positively terminated oxide tip, electrostatic forces dominate the interaction and therefore are larger for the more ionic surfaces. This means that the forces for the two different tips are comparable in magnitude, similar in origin, but differ completely in their hierarchy across the various materials, i.e., the largest force for a silicon tip is over TiO_2, but this provides the smallest force for an oxide tip.

At this point it is interesting to compare the results calculated here for silicon tip interacting with insulating surfaces to similar previous studies of semiconducting surfaces and metallic surfaces. In theoretical studies of Si(111),[19] GaAs(110),[14] InP(110),[16] and Cu(001) (Ref. 37) surfaces using a Si tip, the dominating contrast mechanism in each case was the formation of covalent bonds between the tip apex and the surface. For the binary semiconductors, interaction with the anions in the surface dominated, as in our calculations for insulators. The magnitude of forces found on those surfaces was also comparable, with a maximum of about 2.5 nN over the rest atom in Si, and about 1.5 nN over P in InP and As in GaAs. This implies that the contrast mechanism for a silicon tip with a single dangling bond is universal for all surfaces regardless of physical and electronic structures.

The one serious limitation in studying and controlling the surface electronic structure is that it requires the tip to remain consistent in composition and shape throughout the experiment. If it becomes contaminated during an experiment then it will be difficult to compare results before and after. We have suggested the idea of using applied voltage during an AFM experiment to provide chemical information when the tip is unknown. We should comment here that the method used to calculate the effects of an applied bias does suffer from several approximations. First, and most significantly, it is very difficult to translate the electrostatic fields applied across our unit cell to the bias applied in a real experiment. Although the numbers in principle agree, the real nanoscale bias in experiment where the voltage is applied between the back of the sample and top of the tip separated by a distance of millimeter, is impossible to establish. Second, our calculations are performed at equilibrium, so no charge is allowed to flow out of the cell and the particle numbers are conserved. In principle, for the small amount of charge flowing, this should be a good estimate, but a more accurate method would connect the system to electrodes and allow a real current to flow.

In summary, we see that, although the hierarchy of forces is different for the two tip models, all would provide immediate image interpretation. Therefore the most crucial concern is how to prepare a controlled tip in the first place. Although a positive (or negative) potential oxide tip would offer easy interpretation of insulators, it is very difficult to

imagine a consistent way to control the electrostatic potential at the apex. Since the tips are originally silicon, a more fruitful technique would be just to clean (and keep clean) the tip, hence images would always show brightest contrast over the highest anions in the surface. Combined with the fact that silicon tips also provide equivalent contrast on semiconducting and metallic surfaces this would be an enormous step forward in the development of noncontact AFM.

ACKNOWLEDGMENTS

This research was supported by the Academy of Finland through its Center of Excellence Program (2000-2005). We are grateful to the Center of Scientific Computing (CSC), Espoo for computational resources. A.Y.G. and A.L.S. are grateful to the Engineering and Physical Sciences Research Council (EPSRC) for funding.

[1] *Noncontact Atomic Force Microscopy*, edited by S. Morita, R. Wiesendanger, and E. Meyer (Springer-Verlag, Berlin, 2002).
[2] W. Allers, A. Schwarz, U.D. Schwarz, and R. Wiesendanger, Rev. Sci. Instrum. **69**, 221 (1998).
[3] M.A. Lantz, H.J. Hug, P.J.A. van Schendel, R. Hoffmann, S. Martin, A. Baratoff, A. Abdurixit, H.J. Güntherodt, and C. Gerber, Phys. Rev. Lett. **84**, 2642 (2000).
[4] R. Hoffmann, M.A. Lantz, H.J. Hug, P.J.A. van Schendel, P. Kappenberger, S. Martin, A. Baratoff, and H.J. Güntherodt, Appl. Surf. Sci. **188**, 238 (2002).
[5] T. Eguchi and Y. Hasegawa, Phys. Rev. Lett. **89**, 266105 (2002).
[6] R. Hoffmann, C. Barth, A.S. Foster, A.L. Shluger, H.J. Hug, H. J. Güntherodt, R.M. Nieminen, and M. Reichling (unpublished).
[7] R. Hoffmann, L.N. Kantorovich, A. Baratoff, H.J. Hug, and H. J. Güntherodt (unpublished).
[8] A.S. Foster, C. Barth, A.L. Shluger, and M. Reichling, Phys. Rev. Lett. **86**, 2373 (2001).
[9] A.S. Foster, C. Barth, A.L. Shluger, R.M. Nieminen, and M. Reichling, Phys. Rev. B **66**, 235417 (2002).
[10] A.I. Livshits, A.L. Shluger, A.L. Rohl, and A.S. Foster, Phys. Rev. B **59**, 2436 (1999).
[11] R. Pérez, M.C. Payne, I. Stich, and K. Terakura, Phys. Rev. Lett. **78**, 678 (1997).
[12] S.H. Ke, T. Uda, and K. Terakura, Phys. Rev. B **65**, 125417 (2002).
[13] A.S. Foster, O.H. Pakarinen, J.M. Airaksinen, J.D. Gale, and R.M. Nieminen (unpublished).
[14] S.H. Ke, T. Uda, R. Pérez, I. Stich, and K. Terakura, Phys. Rev. B **60**, 11 631 (1999).
[15] S.H. Ke, T. Uda, I. Stich, and K. Terakura, Phys. Rev. B **63**, 245323 (2001).
[16] J. Tóbik, I. Stich, R. Pérez, and K. Terakura, Phys. Rev. B **60**, 11 639 (1999).
[17] J. Tóbik, I. Stich, and K. Terakura, Phys. Rev. B **63**, 245324 (2001).
[18] A.S. Foster, A.Y. Gal, Y.J. Lee, A.L. Shluger, and R.M. Nieminen, Appl. Surf. Sci. **210**, 146 (2003).
[19] R. Pérez, I. Stich, M.C. Payne, and K. Terakura, Phys. Rev. B **58**, 10 835 (1998).
[20] J. Junquera, O. Paz, D. Sánchez-Portal, and E. Artacho, Phys. Rev. B **64**, 235111 (2001).
[21] J.M. Soler, E. Artacho, J.D. Gale, A. García, J. Junquera, P. Ordejón, and D. Sánchez-Portal, J. Phys.: Condens. Matter **14**, 2745 (2002).
[22] J.P. Perdew, K. Burke, and M. Ernzerhof, Phys. Rev. Lett. **77**, 3865 (1996).
[23] S.G. Louie, S. Froyen, and M.L. Cohen, Phys. Rev. B **26**, 1738 (1982).
[24] D.H. Gay and A.L. Rohl, J. Chem. Soc., Faraday Trans. **91**, 925 (1995).
[25] A.L. Shluger, A.L. Rohl, D.H. Gay, and R.T. Williams, J. Phys.: Condens. Matter **6**, 1825 (1994).
[26] A. Pavese, M. Catti, S.C. Parker, and A. Wall, Phys. Chem. Miner. **23**, 89 (1996).
[27] M. Matsui and M. Akaogi, Mol. Simul. **6**, 239 (1991).
[28] S.L.S. Stipp, Geochim. Cosmochim. Acta **63**, 3121 (1999).
[29] A.L. Rohl, K. Wright, and J.D. Gale, Am. Mineral. **88**, 921 (2003).
[30] M. Cardona and G. Harbeke, Phys. Rev. **137**, A1467 (1965).
[31] D.R. Baer and D.L. Blanchard, Appl. Surf. Sci. **72**, 295 (1993).
[32] R.T. Poole, J. Szajman, R.C.G. Leckey, J.G. Jenkin, and J. Liesegang, Phys. Rev. B **12**, 5872 (1975).
[33] D.M. Roessler and W.C. Walker, Phys. Rev. **159**, 733 (1967).
[34] A.S. Foster, A.L. Shluger, and R.M. Nieminen, Appl. Surf. Sci. **188**, 306 (2002).
[35] J. Neugebauer and M. Scheffler, Phys. Rev. B **46**, 16 067 (1992).
[36] A.L. Shluger, L.N. Kantorovich, A.I. Livshits, and M.J. Gillan, Phys. Rev. B **56**, 15 332 (1997).
[37] I. Štich, P. Dieška, and R. Pérez, Appl. Surf. Sci. **188**, 325 (2002).